# COMPOSITES OF POLY(METHYLMETHACRYLATE) AND MULTI-WALLED CARBON NANOTUBES BY MELT BLENDING

**Caroline McClory[1], Tony McNally[1*], Werner Blau[2], Manuel Ruether[2] and Petra Pötschke[3]**

*[1]Queens University, Belfast, U.K. - c.mcclory@qub.ac.uk [1*]Materials Research Group, School of Mechanical and Aerospace Engineering, Ashby Building, Queens University, Belfast, U.K., BT9 5AH – t.mcnally@qub.ac.uk [2]Trinity College Dublin, Ireland - wblau@tcd.ie [2]Trinity College Dublin, Ireland - ruetherm@tcd.ie [3]Leibniz-Institut für Polymerforschung Dresden e. V.- poe@ipfdd.de*

**Abstract**

Composites of poly (methyl methacrylate) (PMMA) and different multi-walled carbon nanotube types, functionalised versus unfunctionalised, arc-discharge versus CVD at loadings between 0.01 and 10wt.% were prepared by melt compounding using a twin screw extruder. The morphology of the composites was investigated using a range of techniques including scanning electron microscopy (SEM), high resolution transmission electron microscopy (HRTEM) and wide angle X-ray diffraction (WAXD). Raman spectroscopy was used to probe the interactions between matrix and nanotubes. The percolation thresholds (based on viscosity) of each of the blends was determined and related to electrical resistivity measurements.

## Introduction

Carbon nanotubes, since their discovery in 1991, together with fullerenes have been studied intensely due to their unusual properties and their potential to perform in a growing number of useful applications. Carbon nanotubes were identified in 1991 by the electron microscopist Sumio Iijima of NEC Laboratories in Japan.[1] He was investigating the surface of carbon electrodes used in an electric arc-discharge apparatus that had been used to make fullerenes. Carbon nanotubes can be single, double or multi-walled depending on the number of concentric graphitic layers present in each tube. Nanotube diameters are 1000 times smaller than conventional carbon or glass fibres and only an order of magnitude larger than typical polymer molecules.[2] The structure, morphology and properties of nanotubes vary with chosen route of synthesis and nanotube functionality. Compared with carbon fibres, which typically have a Young's modulus of up to 750GPa, the elastic modulus of carbon nanotubes has been measured to be ~1-2TPa.[3,4] The thermal conductivity may be twice that of diamond and electrical conductivity may be 1000 times that of copper wire.[5]

The interest in the area of polymer/CNT composites is immense and has increased dramatically since 1994 when P.M. Ajayan et al. published the first introduction to the area of polymer-nanotube composites.[6] The work was concerned with the alignment of carbon nanotubes embedded in an epoxy matrix. Today, carbon nanotube filled plastics are currently under intensive investigation for enhancement of structural, stress-recovery, electrical and thermal performance while maintaining processibility and deformability of the matrix resin.[7] Melt-mixing[8,9] solution-casting[10] and in-situ polymerisation[11] have all been employed for CNT-polymer composite synthesis. Uniform dispersion and good nanotube/polymer wetting and adhesion are critical factors in the production of composites with enhanced final properties. Nanotube dispersion can be aided by low-impact ball milling[12], the use of surfactants[13], ultrasonic vibration[14,15] and surface functionalisation by means of acid[16] or plasma[17] treatments.

A few previous studies describe the melt-mixing of PMMA, an amorphous engineering polymer, with carbon nanotubes. An early study by Jin et al. in 2001 described how up to 26 wt. % arc discharge MWCNTs were dispersed in PMMA using a laboratory mixing moulder at 200°C.[18] TEM revealed the nanotubes to be undamaged by the mixing process and relatively well dispersed with no large agglomerations present. The nanotubes were found to delay the onset of thermal degradation and the addition of 26 wt.% displayed a 27-fold improvement in storage modulus at 120°C. Gorga and Cohen dry blended PMMA with SWCNTs and MWCNTs before extruding the mixtures at 130°C through a cylindrical die.[19] Good dispersion was achieved at low nanotube loadings and successful alignment of nanotubes was observed by melt drawing the extrudate. An increase in tensile toughness of 170% was achieved with the addition of 1 wt. % orientated MWCNTs with respect to the original polymer. Haggenmueller et al. used a combination of solvent casting and melt mixing to prepare PMMA/SWCNT films and fibres for electrical and mechanical testing.[20] Cast films were repeatedly broken and compression moulded up to 25 times. Optical micrographs revealed the dispersion improved with each cycle, although nanotube bundles still remained. The electrical conductivity along the direction of flow during compression moulding was found to increase from 0.118 to 11.5 S/m as the nanotube loading increased from 1.3 to 6.6 wt. % respectively. Measurements made normal to the direction of flow were significantly lower. The elastic modulus and yield strength of the highly PMMA/SWCNT melt spun fibres increased with nanotube loading and draw ratio.

Functionalisation of the nanotube surface has been used as a method of improving compatibility of the MWCNT and the polymer. Zhou et al. directly modified the surface of MWCNTs with PMMA, then made a range of

composites by further melt-mixing with PMMA.[21] The rheological percolation threshold was reduced from 2.5 wt. % to 1.5 wt. % by using PMMA-modified MWCNTs. Jin et al. used PVDF to bridge the gap between MWCNTs and PMMA.[22] The storage modulus doubled at 50°C by incorporating a small amount (0.5 wt. %) of PVDF.

Oscillatory melt rheology, as reported in the literature[23,24] is often used to detect the frequency dependence of storage modulus and complex viscosity at low frequencies. At a particular nanotube loading, these values can change notably, signifying a rheological percolation threshold due to polymer-nanotube interactions. Here we report the fabrication of PMMA/MWCNT composites by direct melt-mixing. Arc discharge, CVD and functionalised MWCNTs are observed within the polymer matrix and the dispersion assessed. The rheological behaviour of the composites is investigated and the effect of nanotube type on dispersion, rheological and electrical properties is discussed.

## Experimental

*Materials*

The PMMA used in the study was Diakon™ CMG302 supplied by Distrupol Ireland and produced by Lucite International Inc with MFI = 4.4 g /10min (200ºC/5.0kg) (ISO 1133) and ρ=1.18 g/cm$^3$ (ISO 1183). A range of multi-walled carbon nanotube (MWCNT) materials were supplied by a number of companies and academic institutions. Trinity College, Dublin, Ireland used the arc-discharge (AD) route to supply a low purity (15 wt. %) carbon nanotube (CNT) material. These MWCNTs had diameters ranging from 2-10nm and up to 1µm in length. Three other commercially available products were used. The Materials & Electrochemical Research Corp, Tucson, U.S.A. supplied MWCNTs prepared by the arc-discharge method yielding a material with 30-40 wt. % nanotube content. Impurities consist of buckyonions and graphitic particles. The solid cathode deposit material is ground and sieved to particle sizes of <53µm. Each MWCNT has 8-30 graphene layers, 6-20 nm in diameter and 1-5 microns in length. It is reported that powder density is approximately 0.7g/cc. MWCNTs prepared by a catalytic chemical vapour deposition (CCVD) process using acetylene as the carbon source and Fe and Ni as supporting catalysts were supplied by Sun Nanotech® Ltd, People's Republic of China. The final product yielded MWCNTs > 85% pure, diameters within the range 10-30nm and lengths within the range 1-10µm. Nanocyl S.A. Belgium supplied MWCNTs initially synthesised by the CCVD method (95% carbon content) and subsequently functionalised by a Nanocyl patented process to produce MWCNTs with <4% carboxyl (-COOH) functionalisation. The functionalised nanotubes (*f*-CNTs) produced are approx. 10nm in diameter and <1 µm in length. The CNTs were used as received.

*Nanocomposite Preparation*

PMMA and MWCNTs were dried at 80ºC for 24 hrs before processing. Pelletised and ground PMMA was melt blended with up to 10 wt. % MWCNTs using a Dr Collins ZK25 (30:1 L:D ratio) intermeshing co-rotating twin screw extruder. Nanotube loadings of 0.01, 0.05, 0.1, 0.3, 0.5, 1.0, 3.0, 5.0 wt. % were used in all PMMA/MWCNT composites with the exception of PMMA/CVD composites, where ground PMMA (PMMAg) and pelletised PMMA was used to fabricate up to 10 wt. % loaded samples. The average screw speed and temperature during processing were 100rpm and 210°C for all compositions. Circular polymer samples of thickness 250µm and 60mm diameter and also 1.5mm thick and 25mm diameter were hot compression moulded from pelletised extrudate for resistivity and rheological testing respectively.

*Characterisation*

WAXD spectra were recorded using a Siemens D5000 diffractometer using Cu Kα radiation (λ=1.5406Å). HRTEM characterisation was carried out using a Phillips TECNAI F-20 bright field transmission electron microscope at an operating voltage of 200kN. In preparation, samples of approximately 90nm thin were microtomed using diamond knives from extrudate using an Ultracut-E Reichert Jung ultramictrotome. Raman Spectra were collected using an Avalon Instruments Raman Station R1 fitted with an 8200 Detector Element Echelle CCD detector. The system was capable of collecting spectra over a Raman shift spectral range of approximately 250-3500cm$^{-1}$. Volume resistivity measurements were performed on a Keithley Model 6517A electrometer using a Keithley Model 8009 resistivity test fixture. Melt rheological properties of the samples were determined using an ARES-rheometer (Rheometrics Scientific). The measurements were performed in dynamic mode using 25mm parallel plate geometry and a constant gap width of approx. 1.5mm under a liquid nitrogen atmosphere. A constant temperature of 220°C was maintained throughout. Rheological properties were measured as a function of angular frequency which was varied from 0.1 to 100rad/s. The strain amplitude was chosen to be within the viscoelastic range of the polymer.

## Results and Discussion

*Wide-Angle X-ray Diffraction Analysis (WAXD)*

Figure 1 compares the diffraction pattern of composites of PMMA and (a) CVD MWCNT and (b) arc discharge MWCNTs. The characteristic diffraction peak for CVD MWCNTs occurs at a scattering angle of 2θ = 26.1º and 26.2º for arc discharge tubes used in this study. These values are derived from the ordered arrangement of the concentric

cylinders of graphitic carbon. The peak corresponding to the catalytically grown nanotubes in Figure 1(a) disappears on formation of PMMA/CVD MWCNT composites, even at the highest loading. The peak disappears due to the randomly orientated arrangement of nanotubes in the polymer matrix. No short range order remains. The existence of residual catalyst particles is evident from the small peaks at the higher scattering angles. Figure 1(b) however, on examination contains purely carbon material. As the nanotube loading increases, the short range order of the arc discharge tubes is evident even at low loadings (0.3 wt. %). The highly crystalline tubes retain their short range order, even after melt-processing. These rigid, rod-like tubes can be seen clearly in Figure 3(a).

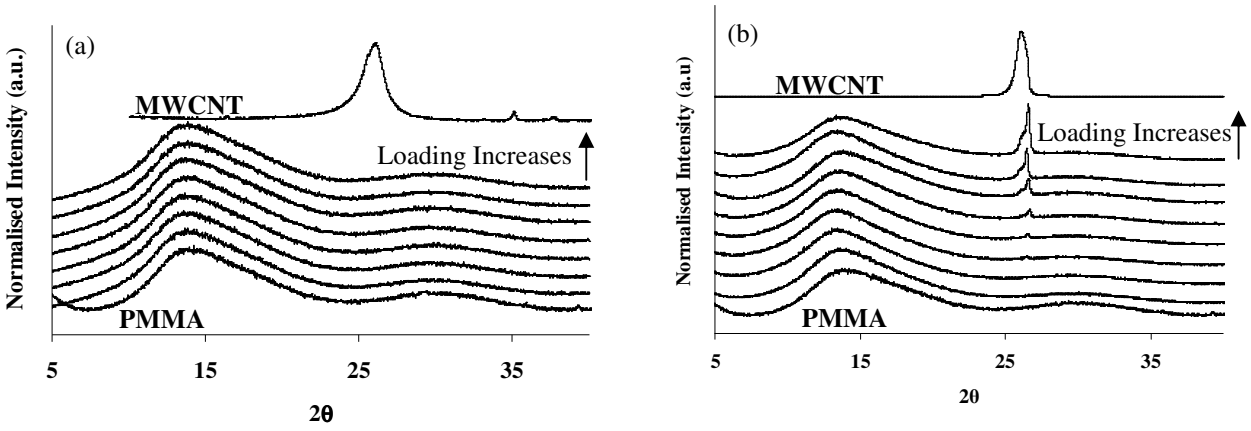


**Figure 1**. WAXD pattern of PMMA/MWCNT Composites (a) PMMA/CVD MWCNTs. (b) PMMA/short Arc Discharge MWCNTs

*Raman Spectroscopy*

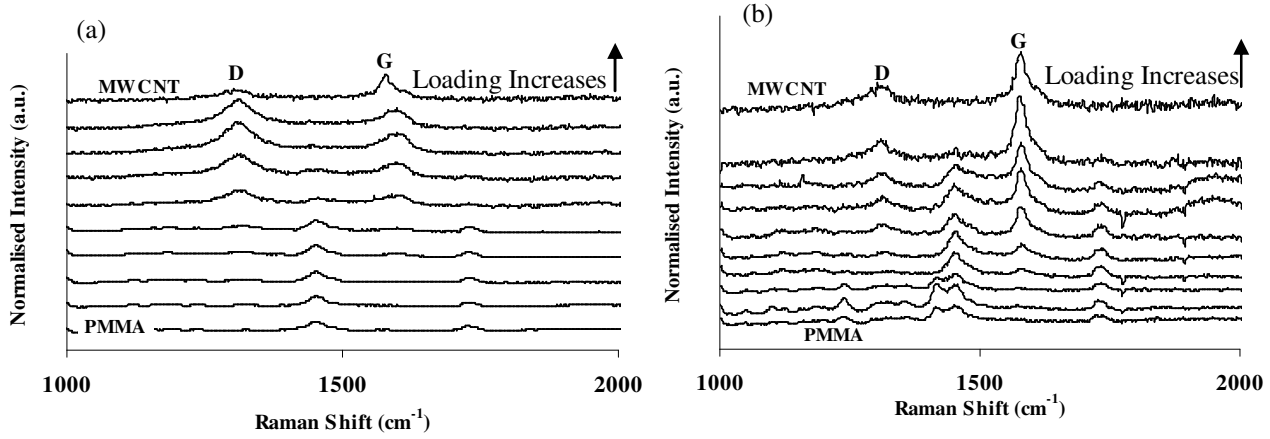


**Figure 2**. Raman Spectra of PMMA/MWCNT Composites (a) PMMA/CVD MWCNTs. (b) PMMA/short Arc Discharge MWCNTs

Figure 2 compares the Raman spectra of composites of PMMA and (a) CVD MWCNT and (b) short arc discharge MWCNTs focusing on the Raman spectrum from 1000cm-1 to 2000cm-1. Raman spectroscopy was used to probe the interactions between the PMMA matrix and MWCNTs. Surface-surface stresses can be incurred by the addition of MWCNTs to a polymeric material. These interfacial interactions can be detected by changes in characteristic features of the Raman spectra of pristine nanotubes. These characteristic peaks occur at 1314 $cm^{-1}$ and 1582 $cm^{-1}$, representing the D (disorder induced) and G (tangential mode) bands respectively. The Raman frequency, intensity and band shape of the vibrations can vary when nanotubes interact with other species. Generally, the interaction between nanotube and polymer is reflected by a peak shift or a peak width change.[25] The addition of 5.0 wt. % CVD MWCNTs to the PMMA induces a shift in the tangential mode (G-band) located at 1582$cm^{-1}$. The peak broadens and an up-shift of 20$cm^{-1}$ is recorded. This peak shift is evident beginning at 0.5 wt.% loading of nanotubes. As previously reported by Dieckmann et al. in a peptide/SWCNT study, changes observed in the nanotube tangential mode (G-band) emphasised the polymer was coating the individual nanotubes in the polymer/CNT composite.[26] This would indicate good surface wetting and therefore good interfacial adhesion between the PMMA and MWCNTs. The addition of 5.0 wt. % short arc discharge

MWCNTs to the PMMA induced a down-shift in the tangential mode. The peak narrowed, increased in intensity and a down-shift of 6cm$^{-1}$ was recorded. This peak shift was evident beginning at 0.3 wt. % loading of nanotubes. The down-shift of the tangential mode is related to charge relationships and electron transfer from tube to polymer but as yet it is not fully understood.

*High Resolution Transmission Electron Microscopy*

Figure 3(a) shows the rigid, rod-like form of the long arc-discharge nanotubes within the PMMA matrix. No large agglomerations were present throughout the entire sample, which contained small amounts of other carbonaceous material in comparison to the samples in Figure 3(b). It was obvious from examination of sample 3(b) that it contained only 15 wt. % of CNT structures within the carbon filler material. Random areas contained large amounts of amorphous carbon and other graphitic structures. Figure 3(c) shows a composite of CVD CNTs and PMMA (in powdered form). These nanotubes are of much higher nanotube purity (~95%). Due to the strong van der Waals forces existing between tubes, agglomeration is common. Some disentanglement of peripheral tubes exists. The image of the *f*-CNT/PMMA composite in Figure 3(d) displays uniform dispersion and a degree of alignment of the *f*-CNTs within the polymer matrix. This alignment may be due to either the extrusion process, the cutting action of the ultramicrotome diamond knife or the repulsion of – COOH functional groups positioned at the end-caps of each tube.

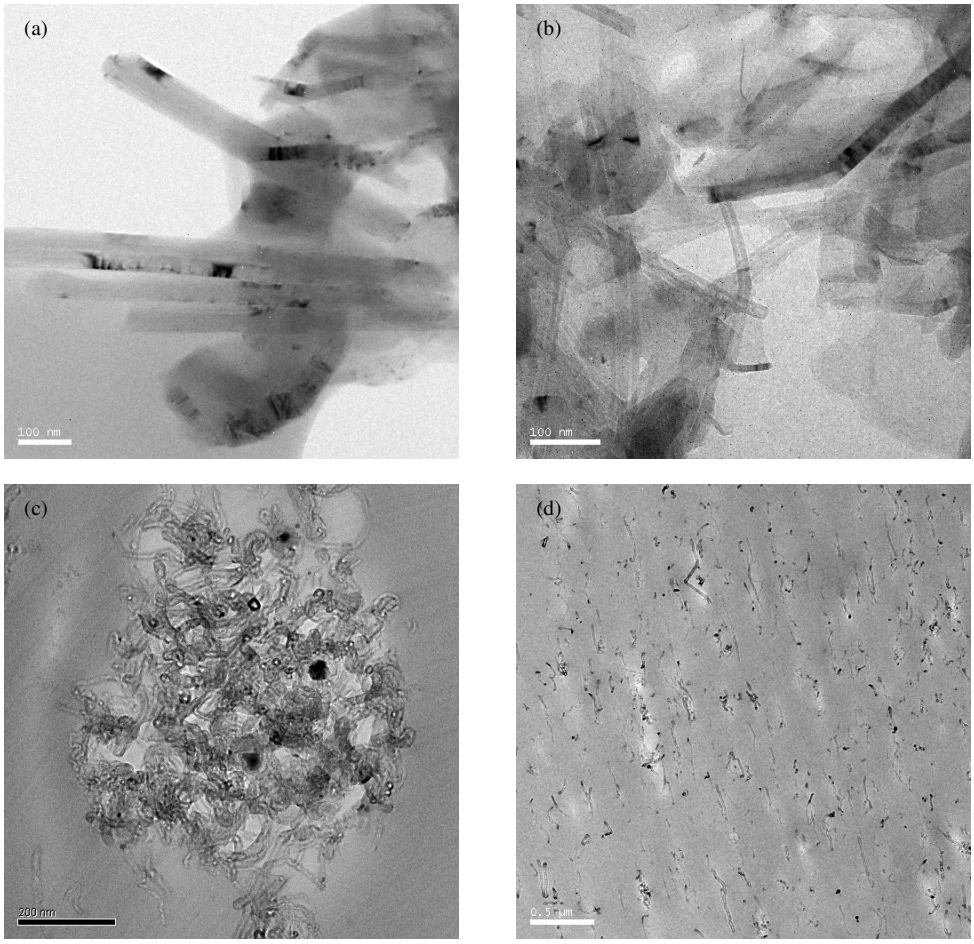


**Figure 3**. TEM images of PMMA composites using (a) 3.0 wt.% long AD CNTs (b) 3.0 wt.% short AD CNTs (c) 5.0 wt.% CVD CNTs and (d) 3.0 wt.% *f*-CNTs.

*Parallel Plate Rheology*

It is well understood that during melt rheology, behaviour at low frequencies is responsive to the changing structure of filled polymer composites. The percolation state of the nanotubes can be detected by a sudden increase in modulus or viscosity as the behaviour of the material becomes less dependent on frequency as the filler loading increases. Viscoelastic properties, storage modulus (G′) and complex viscosity |η*| of 5 and 10 wt. % samples at a constant temperature of 210°C are presented in Figures 4(a) and (b) in the form of log-log plots. The samples with the highest

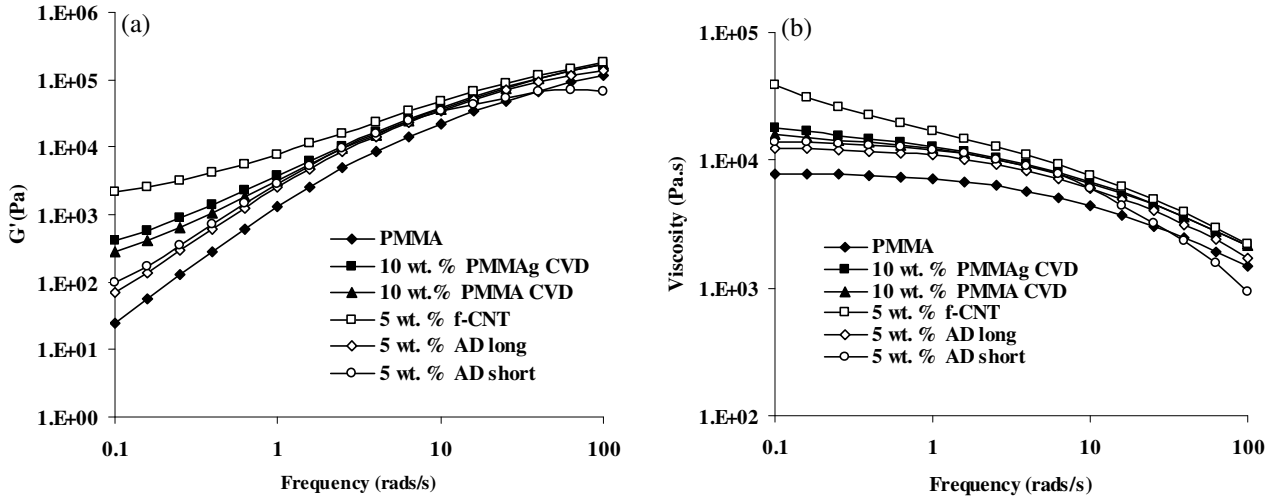


**Figure 4**. (a) Storage modulus (G′) and (b) complex viscosity (Pa.s) versus frequency for PMMA and a range of PMMA/MWCNT composites at the highest CNT loadings.

loading of nanotubes were chosen to represent each composite range. It is apparent that the addition of nanotubes increased G′, especially at low frequencies. Also, the addition of nanotubes increased the complex viscosity of PMMA as would be expected with any filled system. On examination of complex viscosity, the functionalised nanotubes exhibit a constant shear thinning effect during the entire frequency sweep, whereas the neat PMMA is independent of frequency at low values. The complex viscosity of the intermediate composites decreases slightly up to 1 rad/s with 10 wt. % PMMAg/CVD the most viscous. At 210°C and low frequencies PMMA chains are able to relax and respond to sudden increases in speed of oscillation. The presence of nanotubes (above a particular loading) restricts this motion, hindering the relaxation of polymer chains. The result is G′ becomes almost independent of frequency, indicating the polymer is experiencing liquid to solid-like viscoelastic behaviour. The loading during which this transition occurs is known as the rheological threshold.

G′ increases by two decades on addition of 5 wt. % *f*-CNTs. The rheological percolation threshold of *f*-CNTs in PMMA occurs between 3 and 5 wt. % CNTs and is denoted by a sharp increase in G′ between loadings (not shown here). The excellent dispersion of the functionalised tubes and promoted polymer-nanotube interactions due to tube functionality has lead to the formation of a polymer nanotube network. The shear modulus of the CVD CNTs increases by one order of magnitude after the addition of 10 wt. % MWCNTs to both ground and pelletised PMMA although the composites fabricated from the powdered polymer experience the increase to a greater degree. The arc discharge MWCNTs seem to have the least effect on the rheological behaviour of PMMA. It is clear from Figures 4(a) and (b) catalytically grown MWCNTs both functionalised and unfunctionalised impart a greater influence over the structure of the composites.

*Volume Resistivity*

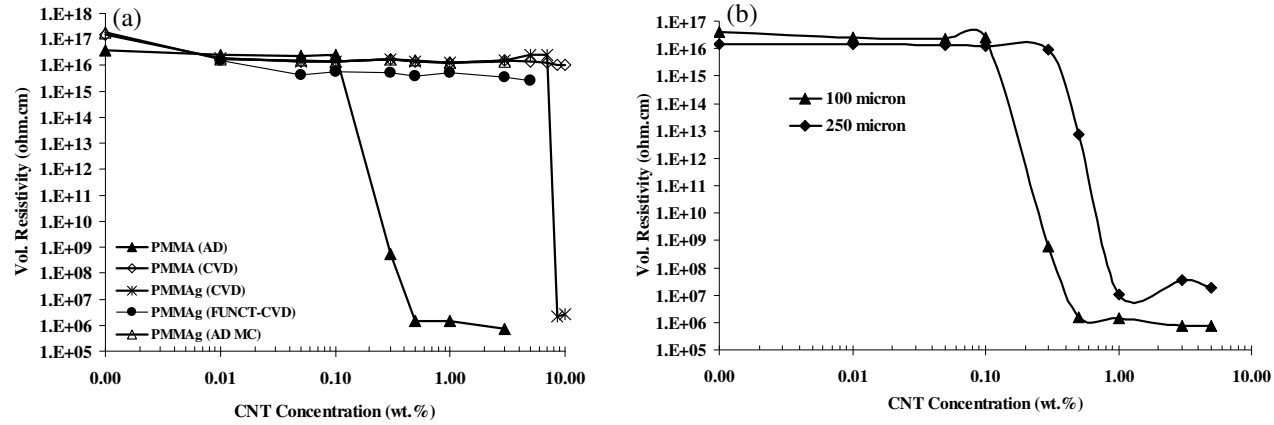


**Figure 5**. (a) Volume resistivity versus CNT loading of various PMMA/CNT composites (b) Comparison of the effect sample thickness has on volume resistivity of PMMA/ long arc discharge MWCNT composites.

The variance of volume resistivity with CNT loading of the various PMMA/CNT composites is displayed in Figure 5(a). The volume resistivity of the PMMA/short arc discharge composite is reduced by 10 orders of magnitude to $7.48E^{+05}$ Ω.cm. Electrical percolation is reached at the threshold value of 0.3 wt. % CNTs. The presence of agglomerations equal to the thickness of the test sample were absent ruling out the risk of short circuiting the test equipment. As the percentage of nanotube material in this sample is quite low, (15 wt. %) the percolating network formed is almost certainly a mixture of MWCNTs, carbon black and other carbon materials. The volume resistivity of the PMMAg/CVD composite is reduced by 10 orders of magnitude to $2.54E^{+06}$ Ω.cm. Electrical percolation is reached at the threshold value of 7.75 wt. % CNTs. Rheological measurement of the same system showed a nanotube-polymer network begins to form at 5 wt. % CNTs. It is interesting to note here that a percolating network of nanotubes is not formed when 10 wt. % CVD MWCNTs are melt-mixed with PMMA in pellet form. Grinding the polymer before the dry-mixing stage and subsequent extrusion encourages dispersion directly from the feed zone as the polymer in powder form takes less time to reach its softening temperature.

The functionalised MWCNTs did not alter the resistivity of the sample. The excellent dispersion achieved did not lead to the formation of a conducting network of nanotubes. Ballistic conductance testing (not reported here) of the *f*-CNTs has proven the nanotubes not to be electrically conductive. The addition of functional groups to a nanotube disturbs its graphitic structure by introducing $sp^3$ carbons to the conjugated system. These $sp^3$ bonded sites are viewed as defects in terms of electron transport through a nanotube. This disruption of the conjugated π-electron system reduces the electrical conductivity of the individual nanotube. Figure 5(b) illustrates the variation in resistivity of PMMA/short arc discharge MWCNTs as the test sample thickness is increased from 100 to 250μm. The percolation threshold increases from 0.3 to 0.5 wt. % as the sample thickness is increased. This is to be expected as the number of electron connections required to form a network of conducting species is greater through the thicker sample.

**Conclusion**

PMMA/MWCNT composites were fabricated by directly melt-mixing untreated MWCNTs with the polymer using twin screw extrusion. Arc discharge, CVD and functionalised MWCNTs are observed within the polymer matrix by TEM. The *f*-CNTs achieved excellent dispersion and a degree of alignment in PMMA. This level of dispersion was consistent throughout the entire sample and attributed to the repulsive forces acting between the functional species on neighbouring tubes. Raman spectroscopy probed polymer-nanotube interfacial interactions demonstrating on average a $20cm^{-1}$ up-shift of the G band relative to the pristine MWCNTs with the exception of the PMMA/short arc discharge CNT composite which experienced an $8cm^{-1}$ down-shift on the addition of just 0.3 wt. % CNTs. The rheological behaviour of the composites was investigated and a rheological percolation threshold was evident for the *f*-CNT/PMMA system between 3 and 5 wt. % *f*-CNTs.

**Acknowledgements**

This work was supported by the EU Specific Targeted Research Project DESYGN-IT (No NMP4-CT-2004-505626). CMcC wishes to thank the Leibniz-Institut für Polymerforschung Dresden e. V. for facilitating a study visit.

**References**

1. S. Iijima, *Nature* 1991, *354*, 56.
2. T.W. Ebbesen, *Carbon Nanotubes*, CRC Press, Boca Raton, Florida, 1997.
3. M.M.J. Treacy, T.W. Ebbesen, J.M. Gibson *Nature* 1996, *381*, 678.
4. O. Lourie, D.M. Cox, H.D. Wagner Phys. Rev. Lett. 1998, *81*,1638.
5. Y. Bin, M. Kitanaka, D. Zhu, M. Matsuo *Macromolecules* 2003, *36*, 6213.
6. P.M. Ajayan, O. Stephan, C. Colliex, D. Trauth *Science* 1994, 265, 1212.
7. H. Koerner, W. Liu, M. Alexander, P. Mirau, H. Dowty, R. Vaia *Polymer* 2005, *46*, 4405.
8. T. McNally, P. Pötschke, P. Halley, M. Murphy, D. Martin, S.E.J. Bell, G.P. Brennan, D. Bien, P. Lemoine, J.P. Quinn *Polymer* 2005, *46*, 8222.
9. A. Bhattacharyya, T. Sreekumar, T. Liu, S. Kumar, L. Ericson, R. Hauge, R. Smalley *Polymer* 2003, *44*, 2373.
10. T. Kashiwagi, F. Du, K.I. Winey, K. Groth, J. Shields *Polymer* 2005, *46*, 471.
11. D. Zilli, C. Chiliotte, M. Escobar, V. Bekeris, G. Rubiolo, A. Cukierman, S. Goyanes *Polymer* 2005, *46*, 6090.
12. A. Kukovecz, T. Kanyó, Z. Kónya, I. Kiricsi *Carbon* 2005, *43*, 994.
13. X. Gong, J. Liu, S. Baskaran, R. Voise, Young *J. Chem. Mater.* 2000, *12*, 1049.
14. S.L. Ruan, P.Gao, X.G.Yang, T.X. Yu *Polymer* 2003, *44*, 5643.
15. X. Jiang, Y. Bin, M. Matsuo *Polymer* 2005, *46*, 7418.
16. J. Sung, H.S. Kim, H. Jin, H.J. Choi, I. Chin *Macromolecules* 2004, *37*, 9899.
17. B. Khare, P. Wilhite, M. Meyyappan *Nanotechnology* 2004, *15*, 1650.
18. Z. Jin, K.P. Pramoda, G. Xu, S.H. Goh *Chem. Phys. Lett.* 2001, *337*, 43.
19. R. E. Gorga, R.E. Cohen *J. Polym. Sci. Part B: Polym. Phys.* 2004, *42*, 2690.
20. R. Haggenmueller, H.H. Gommans, A.G. Rinzler, J.E. Fischer, K.I. Winey *Chem. Phys. Lett*. 2000, *330*, 219.

21. Z. Zhou, S. Wang, L. Lu, Y. Zhang, Y. Zhang *Comp. Sci. & Tech. 2007*, *67*, 1439.
22. Z. Jin, K.P. Pramoda, S.H. Goh, G. Xu *Mat. Res. Bull*. 2002, *37*, 271.
23. F. Du, R.C. Scogna, W. Zhou, S. Brand, J.E. Fischer, K. Winey *Macromolecules* 2004, *37*, 9048.
24. P. Pötschke, T.D. Fornes, D.R. Paul *Polymer* 2002, *43*, 3247.
25. Q. Zhao and H.D. Wagner *Philosophical Transactions of the Royal Society London A: Mathematical, Physical and Engineering Sciences* 2004, *362*, 2407.
26. G.R. Dieckmann, A.B.Dalton, P.A. Johnson, J. Razal, J. Chen, G.M. Giordano, E. Munoz, I. Musselman, R. Baughman, R. Draper *J. Am. Chem. Soc*. 2003, *125*, 1770.